SMC-TR-94-31

AEROSPACE REPORT NO.
TR-92(2925)-5

# Ring Laser Gyro Resonator Design

20 June 1994

Prepared by

R. CHODZKO
Electronics Technology Center
Technology Operations



Prepared for

SPACE AND MISSILE SYSTEMS CENTER
AIR FORCE MATERIEL COMMAND
2430 E. El Segundo Boulevard
Los Angeles Air Force Base, CA 90245



Engineering and Technology Group



THE AEROSPACE CORPORATION
El Segundo California

This report was submitted by The Aerospace Corporation, El Segundo, CA 90245-4691, under Contract No. F04701-88-C-0089 with the Space Systems Division, P. O. Box 92960, Los Angeles, CA 90009-2960. It was reviewed and approved for The Aerospace Corporation by B. K. Janousek, Principal Director, Electronics Technology Center. Jane Christoff, SSD/MJAS was the project officer for the Mission-Oriented Investigation and Experimentation (MOIE) program

This report has been reviewed by the Public Affairs Office (PAS) and is releasable to the National Technical Information Service (NTIS). At NTIS, it will be available to the general public, including foreign nationals.

This technical report has been reviewed and is approved for publication. Publication of this report does not constitute Air Force approval of the report's findings or conclusions. It is published only for the exchange and stimulation of ideas.

WM KYLE SNEDDON, Capt, USAF
Deputy Chief, Industrial & Int'l Div

FRANK PLUM III, Lt. Col, USAF
Deputy Program Manager for DSP

UNCLASSIFIED

SECURITY CLASSIFICATION OF THIS PAGE

## REPORT DOCUMENTATION PAGE

| | |
|---|---|
| 1a. REPORT SECURITY CLASSIFICATION<br>Unclassified | 1b. RESTRICTIVE MARKINGS |
| 2a. SECURITY CLASSIFICATION AUTHORITY | 3. DISTRIBUTION/AVAILABILITY OF REPORT<br>Approved for public release; distribution unlimited |
| 2b. DECLASSIFICATION/DOWNGRADING SCHEDULE | |
| 4. PERFORMING ORGANIZATION REPORT NUMBER(S)<br>TR-92(2925)-5 | 5. MONITORING ORGANIZATION REPORT NUMBER(S)<br>SMC-TR-94-31 |
| 6a. NAME OF PERFORMING ORGANIZATION<br>The Aerospace Corporation<br>Technology Operations<br>6b. OFFICE SYMBOL *(If applicable)* | 7a. NAME OF MONITORING ORGANIZATION<br>Space and Missile Systems Center |
| 6c. ADDRESS *(City, State, and ZIP Code)*<br>El Segundo, CA 90245-4691 | 7b. ADDRESS *(City, State, and ZIP Code)*<br>Los Angeles Air Force Base<br>Los Angeles, CA 90009-2960 |
| 8a. NAME OF FUNDING/SPONSORING ORGANIZATION<br>8b. OFFICE SYMBOL *(If applicable)* | 9. PROCUREMENT INSTRUMENT IDENTIFICATION NUMBER<br>F04701-88-C-0089 |
| 8c. ADDRESS *(City, State, and ZIP Code)* | 10. SOURCE OF FUNDING NUMBERS<br>PROGRAM ELEMENT NO. / PROJECT NO. / TASK NO. / WORK UNIT ACCESSION NO. |

11. TITLE *(Include Security Classification)*
Ring Laser Gyro Resonator Design

12. PERSONAL AUTHOR(S)
Chodzko, R.

| 13a. TYPE OF REPORT | 13b. TIME COVERED FROM ____ TO ____ | 14. DATE OF REPORT *(Year, Month, Day)* | 15. PAGE COUNT |
|---|---|---|---|
| | | 1994 June 20 | 21 |

16. SUPPLEMENTARY NOTATION

| 17. COSATI CODES | | | 18. SUBJECT TERMS *(Continue on reverse if necessary and identify by block number)* |
|---|---|---|---|
| FIELD | GROUP | SUB-GROUP | Ring resonator design, Stable cavities, Ring laser gyroscopes, Resonator misalignment effects |
| | | | |
| | | | |


19. ABSTRACT *(Continue on reverse if necessary and identify by block number)*

Ring laser gyroscopes (RLGs) have been used for navigation on the Atlas II launch vehicle and are scheduled for the Titan IV and Delta launch vehicles. The typical launch vehicle random-vibration environment could cause errors in measured RLG rotation rates due to vibration (tilt) of the resonator mirrors. Vibration-induced mirror tilt can create a variation in laser power due to laser beam occlusion by the intracavity mode control aperture(s). In the present work, we have analyzed the RLG resonator design theoretically and calculated pertinent parameters such as the beam diameter at the aperture, cavity mirror alignment sensitivities, and power loss due to aperture occlusion. The mirror vibration levels required to significantly affect the laser power were then calculated for typical RLG resonator geometries. It is concluded that vibration-induced bending of a typical RLG resonator structure should not cause a significant loss in laser power.


| 20. DISTRIBUTION/AVAILABILITY OF ABSTRACT | 21. ABSTRACT SECURITY CLASSIFICATION |
|---|---|
| [X] UNCLASSIFIED/UNLIMITED [ ] SAME AS RPT. [ ] DTIC USERS | Unclassified |

| 22a. NAME OF RESPONSIBLE INDIVIDUAL | 22b. TELEPHONE *(Include Area Code)* | 22c. OFFICE SYMBOL |
|---|---|---|
| | | |

DD FORM 1473, 84 MAR

83 APR edition may be used until exhausted.
All other editions are obsolete.

SECURITY CLASSIFICATION OF THIS PAGE
UNCLASSIFIED

## PREFACE

I would like to acknowledge the assistance of Drs. J. M. Bernard and W. R. Fenner of the Electronics Technology Center and Dr. H. Mirels of the Mechanics and Materials Technology Center in the preparation of this report. This work was conducted under Contract F04701-88-C-0089 with the Air Force Space and Missile Systems Center.

## CONTENTS



## FIGURES

# 1.0 INTRODUCTION

The purpose of this report is to discuss the optical resonator issues in the design of Ring Laser Gyroscopes (RLGs) used for launch vehicle navigation applications. In the present work, we have analyzed an optical ring resonator geometry that is typical of some existing commercial RLGs. For a stable ring resonator, we have calculated parametrically the laser beam intensity distributions, longitudinal and transverse mode beat frequencies, and mirror alignment sensitivities. In particular, we have analyzed the effect of vibration-induced, out-of-plane tilt of the ring resonator mirrors in reducing the output power of an RLG due to laser beam occlusion by the mode control aperture(s).

We performed a geometric optics analysis of an RLG resonator and determined the change in position of the optical axis due to an angular tilt of one of the cavity mirrors. For small tilt angles, the stable cavity transverse mode retains a Gaussian intensity distribution. From the calculated transverse displacement of the optic axis, we have computed the reduction in the RLG output power due to occlusion by the mode control aperture(s) as a function of mirror tilt angle. The reduction in output power was then related to vibration-induced tilt effects due to bending of the resonator structure.

## 2.0 THEORY

A typical three-mirror resonator design for an RLG is shown in Figure 1. The resonator consists of two flat mirrors (FM1 and FM2) and a concave mirror (CM) with a radius of curvature, R. The distance between the mirror, CM, and either flat is $L_2$ and between FM1 and FM2 is $L_1$. The angle of incidence on the CM is $A_i$ and typically has a large value (20° to 30°). This large angle of incidence on the CM implies that the resonator is astigmatic, with two effective concave radii of curvatures, $R_x$ and $R_y$. Figure 2 shows the theoretical variation of $R_x/R$ and $R_y/R$ with angle of incidence $A_i$. These radii are parallel and perpendicular to the plane of incidence (resonator plane), respectively. The resonator in Figure 1 has the equivalent lens sequence shown in Figure 3, where the reference plane corresponds to the position of the CM. The ABCD matrix for one resonator round trip through the lens sequence in Figure 3 is given by[1,2]

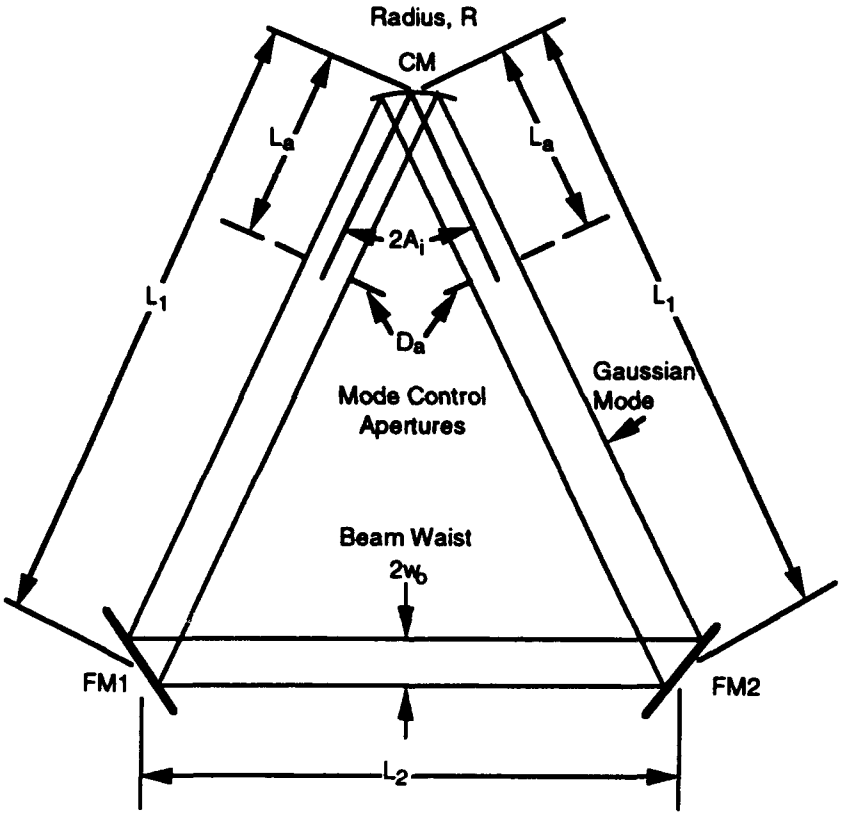


Figure 1. Three-mirror ring laser gyro resonator geometry.

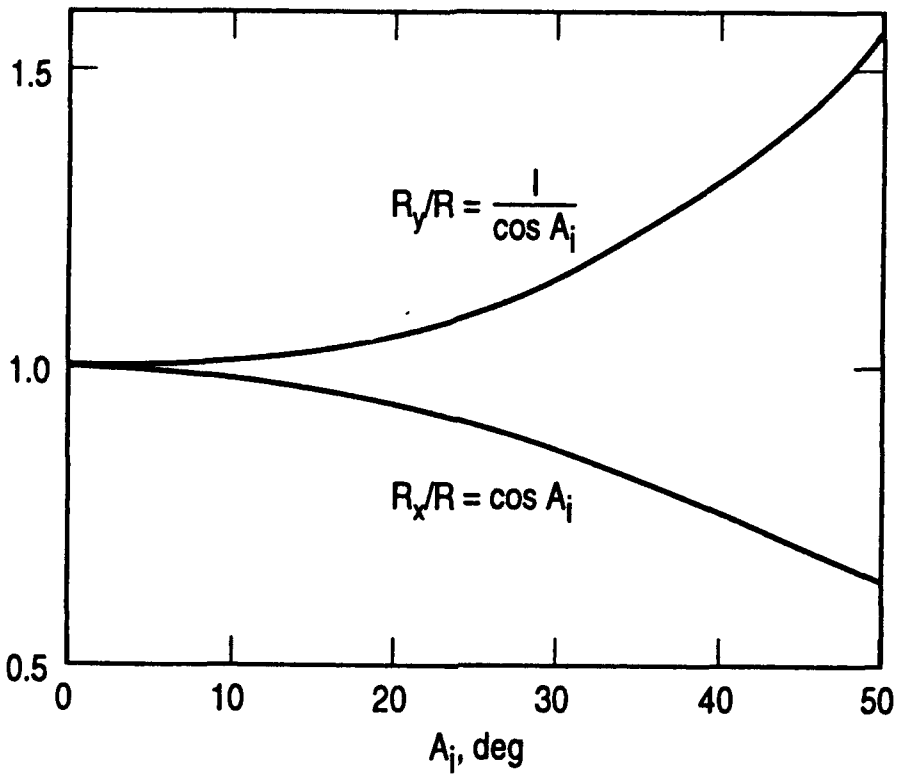


Figure 2. Mirror radii for astigmatic ring resonator.

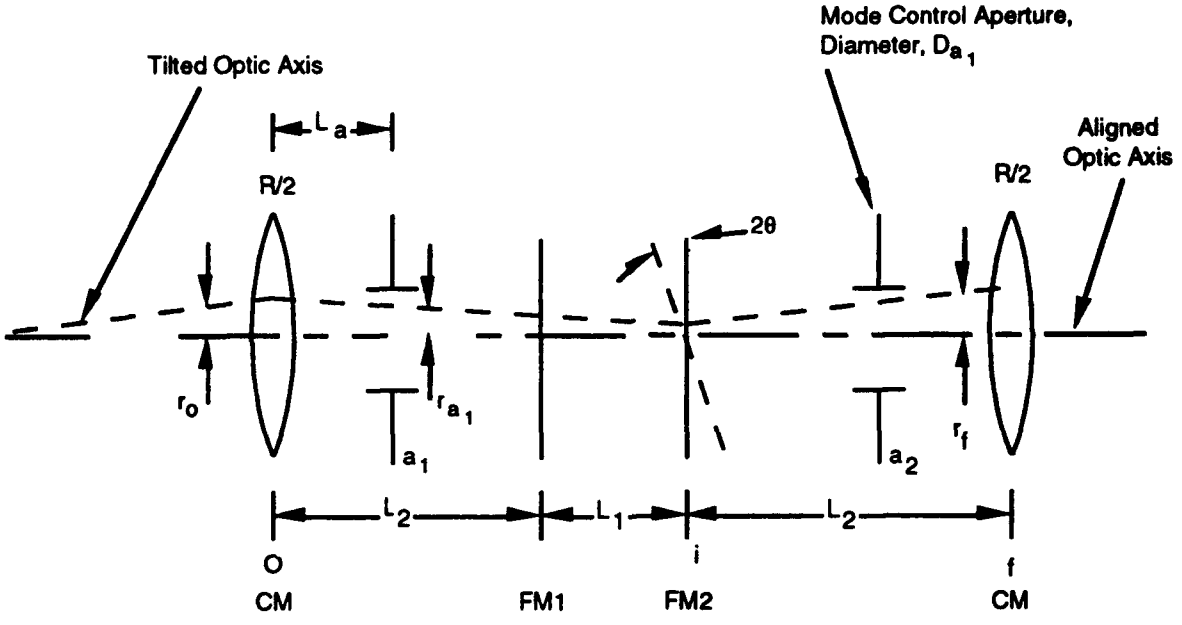


Figure 3. Equivalent lens sequence for ring laser gyro resonator.

$$\begin{pmatrix} A & B \\ C & D \end{pmatrix} = \begin{bmatrix} 1 - \dfrac{2(L_1 + 2L_2)}{R} & (L_1 + 2L_2) \\ -2/R & 1 \end{bmatrix},$$

where the ABCD matrix relates the position (r) and slope (r') of an arbitrary paraxial ray that traverses the optical train.

$$\begin{pmatrix} r_f \\ r_f' \end{pmatrix} = \begin{pmatrix} A & B \\ C & D \end{pmatrix} \begin{pmatrix} r_o \\ r_o' \end{pmatrix}.$$

The ABCD matrix predicts the resonator stability properties, the beam spatial intensity distribution, the radius of curvature of the wavefront, the cavity longitudinal and transverse mode frequencies, and the alignment sensitivity of the cavity mirrors. The resonator stability is given by $m = (A + D)/2 = [1 - (L_1 + 2L_2)/R]$, where $m = 1$ is the boundary of stability. If $|m|$ is less than 1, an off-axis paraxial ray launched within the aligned stable ring resonator will follow a bounded (low diffraction loss), sinusoidal path within the equivalent lens sequence.[2] If $|m|$ is greater than 1, the resonator is unstable and an off-axis paraxial ray will walk out (large diffraction loss) of the equivalent lens sequence. A low-loss, stable ring resonator design is required for a conventional RLG.

## 2.1 BEAM WAIST DIMENSIONS

The $TEM_{oo}$ mode pattern inside a stable ring resonator is a Gaussian intensity distribution with a beam half-width (at the position of the CM in Figure 2) given by[1,2]

$$w^2 = \frac{2\lambda B}{\pi} / \left[4 - (A + D)^2\right]^{1/2}$$

in terms of the ABCD matrix parameters. From the Gaussian beam relation,

$$w_o^2 = w^2 / \left[1 + \left(\frac{\pi w^2}{\lambda R}\right)^2\right],$$

the beam waist, $w_o$, (halfway between FM1 and FM2) can be calculated in terms of the cavity parameters, $L_1$, $L_2$, mirror radius R, and wavelength $\lambda$ as

$$w_o = \sqrt{\lambda L_r/\pi}\left(\frac{2L_r}{R} - \frac{L_r^2}{R^2}\right)^{-1/4}\left(1 - \frac{L_r}{R}\right)^{1/2},$$

where $L_r = L_1 + 2L_2$. Using the relation

$$w_a = w_o\left[1 + \left(\frac{\lambda z_a}{\pi w_o^2}\right)^2\right]^{1/2},$$

where $z_a = L_1/2 + L_2 - L_a$, the beam half-width at the mode control apertures can be calculated.

Figure A1 in the appendix shows the variation of the Gaussian beam waist parameter $w_o/(\lambda L_r/\pi)^{1/2}$ with the resonator parameter $L_r/R$. Thus, when the mirror radius, R, becomes large, the beam waist becomes large for a fixed value of the ring resonator total length, $L_r$. Also plotted is the beam half-width parameter ($w_a/w_o$) for various values of the aperture location parameter $L_a/L_r$, which varies between 0 and 0.5, the latter corresponding to a single aperture at the beam waist. For typical RLG geometries $w_a = w_o$ to within about 5 percent.

## 2.2 RESONATOR BEAT FREQUENCIES

The stable ring resonator longitudinal and transverse mode beat frequencies for typical RLG designs are discussed in the appendix and shown in Figure A2. The astigmatic three-mirror design in Figure 1 leads to transverse mode frequencies associated with the $R_x$ and $R_y$ mirror radii as well as the difference frequency. These beat frequencies could be a source of noise in the RLG output if they were within the bandpass of the detector/amplifier electronics. These beat frequencies can be eliminated by using a mode control aperture within the resonator with a diameter approximately equal to the Gaussian beam width. Reducing the diameter of the mode control aperture for transverse mode control, on the other hand, will increase the alignment sensitivity to resonator mirror tilt.

## 2.3 RESONATOR MIRROR ALIGNMENT SENSITIVITIES

The ray-matrix approach for the RLG resonator can be used to calculate the sensitivity to misalignment of both the flat and concave resonator mirrors. One can calculate the radial position (r) and slope (r') of the optical axis ray at the position of the mode selection aperture. The analysis assumes a small angle (sinr' = r') or paraxial ray approximation. This approximation only applies to rays with a small angle of incidence on the concave resonator mirror, i.e., tilt angles perpendicular to the resonator plane (y direction). Note that for typical RLG resonator designs, $A_i$ = 20° to 30°, and the paraxial approximation does not apply for tilt angles within the resonator plane (x direction). Thus, for the present analysis, only the mirror radius of curvature, $R_y$, will be used to calculate the tilt sensitivity within the paraxial approximation.

We use the approach given by A. Schnurr[3] to calculate the alignment sensitivity of the RLG resonator. Let $r_f$ denote the ray position on the aperture after one round trip through the lens sequence in Figure 2 starting at position $r_0$. Let $r_i$ denote the ray position on FM2 tilted by an

angle $\theta$ in a direction perpendicular to the resonator plane. If the FM2 flat RLG resonator mirror is tilted, the ray matrix equation relating $r_f$ to $r_i$ is given by:

$$\begin{pmatrix} r_f \\ r'_f \end{pmatrix} = \begin{pmatrix} 1 & L_2 \\ 0 & 1 \end{pmatrix} \begin{pmatrix} r_i \\ r'_i + 2\theta \end{pmatrix}$$

The matrix equation relating $r_i$ to $r_o$ is given by:

$$\begin{pmatrix} r_i \\ r'_i \end{pmatrix} = \begin{pmatrix} 1 & L_1 \\ 0 & 1 \end{pmatrix} \begin{pmatrix} 1 & L_2 \\ 0 & 1 \end{pmatrix} \begin{pmatrix} 1 & 0 \\ -\frac{2}{R_y} & 1 \end{pmatrix} \begin{pmatrix} r_o \\ r'_o \end{pmatrix}$$

These two equations, plus the condition that the optical axis ray self-replicates after one round trip, (i.e., $r_f = r_o$, and $r'_f = r'_o$) yield a solution for the FM2 tilt sensitivity. The solution at the position of the mode control apertures $a_1$ and $a_2$ is:

$$r_{a1} = [R_y - 2(L_1 + L_2)L_a/(L_1 + 2L_2)]\theta$$

$$r'_{a1} = 2\theta(L_1 + L_2)/(L_1 + 2L_2)$$

$$r_{a2} = [R_y - 2(L_1 + L_2)(L_2 + L_a)/(L_1 + 2L_2) + 2L_a]\theta$$

$$r'_{a2} = -2\theta[1 - (L_1 + L_2)/(L_1 + 2L_2)] .$$

In a similar manner, the solution for the CM tilt sensitivity can be obtained. The result is $r_{a2} = R_y\theta$, and $r'_{a1} = r'_{a2} = 0$. Thus, tilting the CM translates the optical axis in a direction parallel to its initial direction. It should be noted that tilting FM2 produces a different displacement of the optical axis at apertures 1 and 2. This difference is small, however, for typical resonator design parameters (~2%), and the largest displacement occurs at aperture 1. It can be shown that an optical axis displacement of $r_a = R_y\theta$ is a reasonable approximation (to within 10%) for tilting either the concave or a flat mirror of a typical RLG resonator.

## 2.4 RLG POWER SENSITIVITY TO VIBRATION

Now that the RLG resonator alignment sensitivity characteristics have been determined, the effect of vibration on output power due to occlusion by the mode control aperture can be studied. A calculation was made of the variation in power transmitted through a circular aperture due to a transverse translation of a Gaussian laser beam[4]. This result is shown in Figure A3, where the transmitted power is plotted as a function of beam translation, $r_a$, for various values of $D_a/(2w_a)$, assuming either one or two mode control apertures. Two apertures imply approximately twice as much loss as for a single aperture for a given translation. Figure A3 also shows how decreasing the aperture radius compared to the beam half-width increases the power loss due to translation. A procedure is discussed in the appendix that uses Figures 2, A1, and A3 to calculate the power loss versus mirror tilt angle due to occlusion of the laser beam by the mode control apertures for the three mirror RLG resonator design in Figure 1 with arbitrary parameters, $L_1$, $L_2$, $L_a$, $D_a$, R, and $A_i$.

The variation in resonator output power versus resonator mirror tilt for four typical RLG resonator designs is shown in Figure 4. A critical angle is defined as the tilt angle required to reduce the output power by 20 percent. A vertical line of 50 microradians defines the maximum expected mirror tilt due to flexure of the resonator structure (e.g., Zerodur material) for a 40g acceleration.[5,6] This is the maximum acceleration expected due to random vibrations that could occur in a launch vehicle such as an Atlas II or Titan IV. Design numbers 2, 3, and 4 correspond to some typical RLG designs, and design number 1 corresponds to a hypothetical resonator where significant power degradation due to tilt is expected. Thus, designs 1 and 2 are approximately 14 and 4 times, respectively, more sensitive to tilt than design 4. The most important parameters determining tilt sensitivity for a specific laser wavelength are R, $L_r$, and $D_a$. Critical angles for the three typical RLG designs vary between 140 and 470 microradians. Design number 2, which is the most sensitive to misalignment of these three designs, is still about a factor of 3 from the flexure limit.

DESIGN # RLG RESONATOR DESIGNS, $\lambda = 0.6328\ \mu$

1 $L_r = 15$ cm, R = 5 m, $A_i = 30°$, $D_a = 0.66$ mm, $w_a = 0.33$ mm, 1 APERTURE

2 $L_r = 32$ cm, R = 5 m, $A_i = 25°$, $D_a = 2.16$ mm, $w_a = 0.43$ mm, 2 APERTURE

3 $L_r = 15$ cm, R = 1 m, $A_i = 30°$, $D_a = 1.10$ mm, $w_a = 0.22$ mm, 1 APERTURE

4 $L_r = 32$ cm, R = 1 m, $A_i = 25°$, $D_a = 1.42$ mm, $w_a = 0.28$ mm, 2 APERTURE

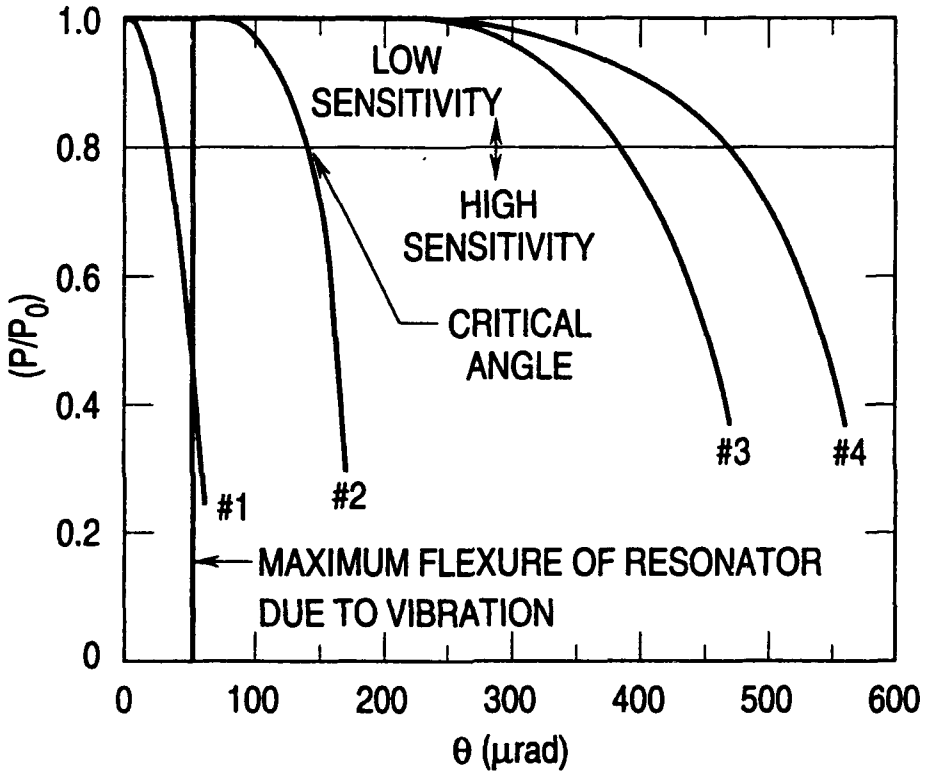


Figure 4. Power loss vs resonator mirror tilt angle due to occlusion by mode control aperture(s).

## 3.0 CONCLUSIONS

In conclusion, we have developed a theoretical model of a three-mirror stable ring resonator consisting of a concave mirror and two flat mirrors applicable to ring laser gyros. This model determines the Gaussian beam sizes, the longitudinal and transverse mode frequencies, and the sensitivity of laser power loss due to occlusion of a mode control aperture by misaligning the resonator mirrors. A geometric optics approach employing ABCD ray matrices was used to calculate the effects of misalignment within the paraxial approximation. A calculation procedure was developed to compare alignment stability of various three-mirror RLG resonator designs. Critical cavity mirror tilt angles were calculated for four RLG resonator designs that reduced the laser power by 20 percent due to mode control aperture occlusion. In addition, the analysis can determine the sensitivity of a given resonator design to the random vibrations within a launch vehicle environment. Typical critical angles of 140 to 470 microradians indicate that resonator block flexure induced by random vibrations (as high as 40g's) is not sufficient to cause a significant variation in laser power. We are curently developing a non-paraxial analysis of tilt effects within the resonator plane (x direction).

## APPENDIX

### BEAM WAIST DIMENSIONS

Figure A1 is a plot of the beam waist half-width and the half-width at the mode control apertures as a function of $L_r/R$ and $L_a/L_r$, respectively (Equations 1 and 2). This plot is required to calculate the power loss due to resonator mirror tilt as discussed below.

### RESONATOR BEAT FREQUENCIES

The formula for the longitudinal and transverse mode frequencies of the RLG stable ring resonator is given by[7]

$$\nu/\nu_o = q + \frac{1}{2\pi}\cos^{-1}(1 - L_r/R_y)\left(n + \frac{1}{2}\right) + \frac{1}{2\pi}\cos^{-1}(1 - L_r/R_x)\left(m + \frac{1}{2}\right),$$

where q, m, and n are integers.

The longitudinal mode frequency spacing is therefore $\nu_o = c/L_r$. The longitudinal and transverse mode frequency spacings are shown in Figure A2 as a function of CM radius of curvature, $R_x$ or $R_y$, for two different cavity lengths, $L_r$, appropriate for typical RLG resonator geometries. It should be noted that mirror radii $R_x$ and $R_y$ due to astigmatism will produce two different transverse-mode frequencies, $\nu_x$ and $\nu_y$, as well as the difference frequency $\nu_x - \nu_y$ in the laser output beam. For example if $A_i = 30°$, R = 5 m, $L_r$ = 30 cm, then from Figure 2, $R_x$ = 4.33 m, $R_y$ = 5.77 m, $\nu_x$ = 60 MHz, $\nu_y$ = 52 MHz, and $\nu_x - \nu_y$ = 8 MHz. The 8-MHz beat frequency could be a source of noise in the laser detector output. These beat frequencies will appear in the laser detector output signal if the mode control aperture is not small enough ($D_a = 2w_o$) to ensure Gaussian $TEM_{oo}$ mode operation.

### RLG POWER SENSITIVITY TO CAVITY MIRROR TILT

Figure A3 is a plot of the variation of the power ($P/P_o$) transmitted through a circular aperture due to the transverse translation ($r_a$) of a Gaussian laser beam.[4] The curves are plotted for various values of the parameter $D_a/(2w_a)$, assuming either one or two apertures. Figures 2, A1, and A3 were used to generate Figure 4.

The calculation procedure is illustrated for the specific example of design No. 2 in Figure 4. Consider a typical RLG resonator design where $L_r$ = 32 cm, $\lambda$ = 0.6328 microns, R = 5 m, $A_i$ = 25°, and two apertures with $L_a/L_r$ = 0.09. From Figure 2, $R_y$ = 5.5 m. The beam waist is determined from Figure A1 for $L_r/R_y$ = 0.058 as $w_o/(\lambda L_r/\pi)^{1/2}$ = 1.68, which yields $w_o$ = 0.427 mm and $w_a$ = 0.433 mm. We can now determine a critical tilt angle to reduce the RLG power by 20% from Figure A3. Assume $D_a/(2w_a)$ = 2.5, which implies an aperture diameter, D, of 2.16 mm. From Figure A3 this gives $2r_a/D_a$ = 0.73 for two apertures. $r_a$ is approximately equal to $R_y\theta$ for either the concave or flat mirrors. This implies a critical tilt angle of $\theta = (2r_a/D_a)D_a/(2R_y)$ = 143 microradians to produce a 20% power reduction.

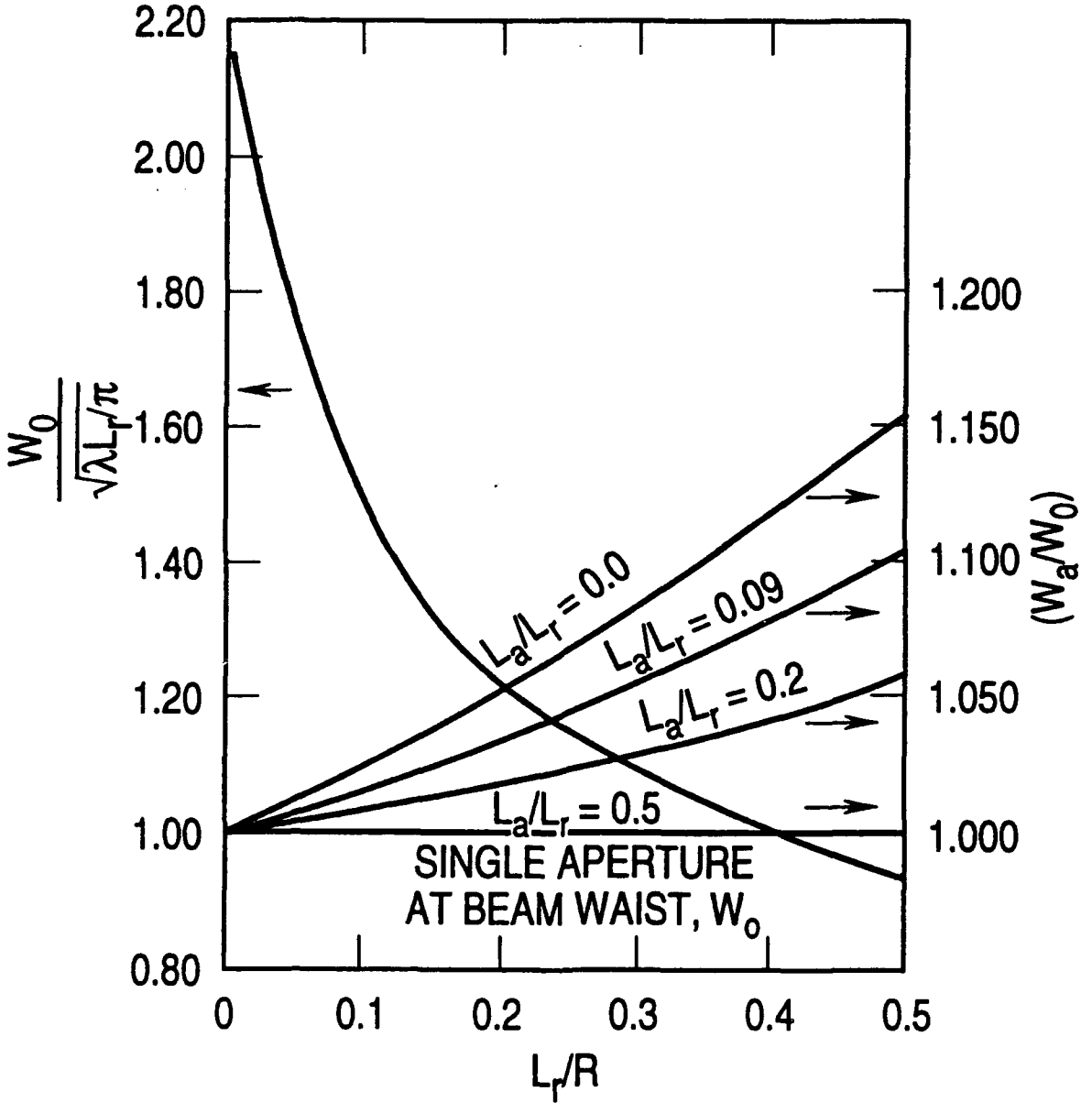


Figure A1. Beam waist ($w_0$) and beam half-width ($w_a/w_0$) at mode control aperture vs resonator parameters, $L_r/R$ and $L_a/L_r$.

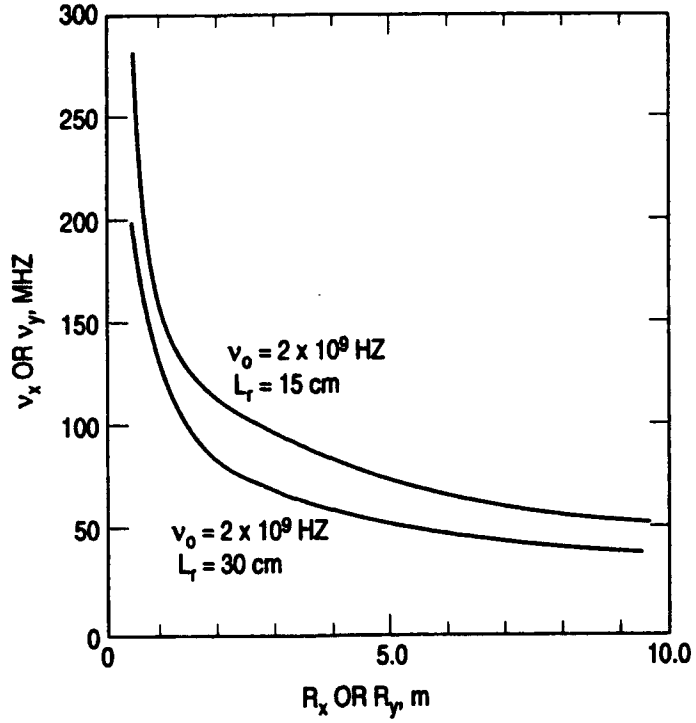


Figure A2. Transverse mode frequency spacing vs mirror radii of curvature.

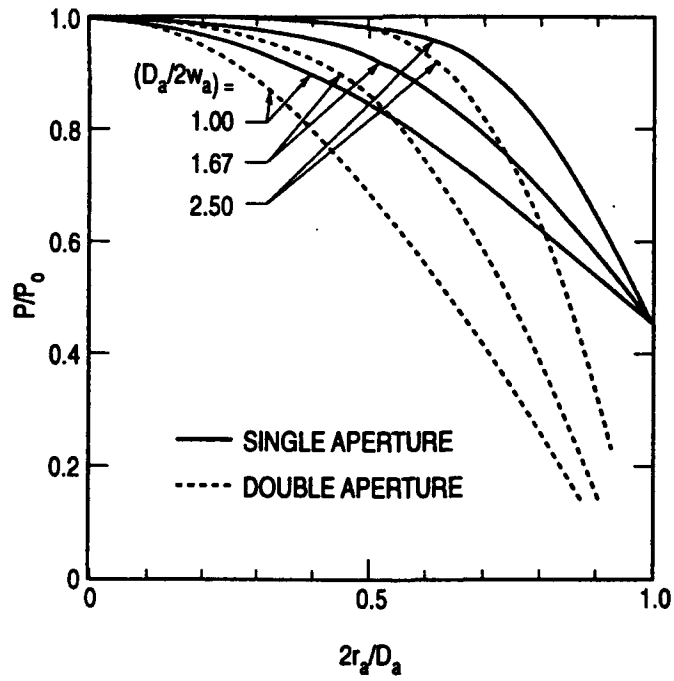


Figure A3. Power transmitted through aperture vs transverse displacement of Gaussian beam.

## 5.0 REFERENCES


1. H. Kogelnik and T. Li, "Laser Beams and Resonators", Proceedings of the IEEE, 54, pp 1312-1329, 1966

2. A. E. Siegman, "Lasers", University Science Books, Mill Valley, California, 1986

3. A. D. Schnurr, "Unstable Resonator Misalignment in Ring and Linear Toroidal Resonators", Applied Optics, 22, pp 298-303, 1983

4. H. Mirels, Private Communications

5. D. Platus, Private Communications

6. R. M. Hohenstein, "Vibration Sensitivity of an RLG: Deflection of the Body", IOC No. A91-5414-RHM-21, 18 March 1991

7. S. A. Collins, Jr., "Analysis of Optical Resonators Involving Focusing Elements", Applied Optics, 3, pp 1263-1275, 1964

## TECHNOLOGY OPERATIONS

The Aerospace Corporation functions as an "architect-engineer" for national security programs, specializing in advanced military space systems. The Corporation's Technology Operations supports the effective and timely development and operation of national security systems through scientific research and the application of advanced technology. Vital to the success of the Corporation is the technical staff's wide-ranging expertise and its ability to stay abreast of new technological developments and program support issues associated with rapidly evolving space systems. Contributing capabilities are provided by these individual Technology Centers:

**Electronics Technology Center:** Microelectronics, solid-state device physics, VLSI reliability, compound semiconductors, radiation hardening, data storage technologies, infrared detector devices and testing; electro-optics, quantum electronics, solid-state lasers, optical propagation and communications; cw and pulsed chemical laser development, optical resonators, beam control, atmospheric propagation, and laser effects and countermeasures; atomic frequency standards, applied laser spectroscopy, laser chemistry, laser optoelectronics, phase conjugation and coherent imaging, solar cell physics, battery electrochemistry, battery testing and evaluation.

**Mechanics and Materials Technology Center:** Evaluation and characterization of new materials: metals, alloys, ceramics, polymers and their composites, and new forms of carbon; development and analysis of thin films and deposition techniques; nondestructive evaluation, component failure analysis and reliability; fracture mechanics and stress corrosion; development and evaluation of hardened components; analysis and evaluation of materials at cryogenic and elevated temperatures; launch vehicle and reentry fluid mechanics, heat transfer and flight dynamics; chemical and electric propulsion; spacecraft structural mechanics, spacecraft survivability and vulnerability assessment; contamination, thermal and structural control; high temperature thermomechanics, gas kinetics and radiation; lubrication and surface phenomena.

**Space and Environment Technology Center:** Magnetospheric, auroral and cosmic ray physics, wave-particle interactions, magnetospheric plasma waves; atmospheric and ionospheric physics, density and composition of the upper atmosphere, remote sensing using atmospheric radiation; solar physics, infrared astronomy, infrared signature analysis; effects of solar activity, magnetic storms and nuclear explosions on the earth's atmosphere, ionosphere and magnetosphere; effects of electromagnetic and particulate radiations on space systems; space instrumentation; propellant chemistry, chemical dynamics, environmental chemistry, trace detection; atmospheric chemical reactions, atmospheric optics, light scattering, state-specific chemical reactions and radiative signatures of missile plumes, and sensor out-of-field-of-view rejection.